RSC Advances

PAPER

View Article Online
View Journal | View Issue

Cite this: *RSC Adv.*, 2017, **7**, 34984

Preparation of a Mg/Al/Fe layered supramolecular compound and application for removal of Cr(VI) from laboratory wastewater

Xuejin Wang,[ab] Xiaping Zhu *[a] and Xingrui Meng[a]

Herein, a Mg/Al/Fe layered supramolecular compound (Mg/Al/Fe-LDH) was fabricated *via* a co-precipitation method with a Mg/Al/Fe mixed solution and used to remove Cr(VI) in laboratory wastewater. The physicochemical properties of the materials were studied using X-ray diffraction patterns, Fourier transform spectra, N_2 adsorption–desorption isotherms, pore size distribution curves, and scanning electron microscopy and X-ray photoelectron spectroscopy images. Mg/Al/Fe-LDH was prepared with the Mg(II) : Fe(II) : Al(III) molar ratios of 5 : 1 : 2 and aged at 80 °C for 24 h. Structural analysis showed that the Mg/Al/Fe-LDH was a layered supramolecular compound. The optimal removal process of calcined Mg/Al/Fe-LDH (Mg/Al/Fe-CLDH) for Cr(VI) was as follows: the pH value was 9–10 and the adsorption process was carried out at room temperature for 100 min. It was found that the saturated adsorption capacity reached 725.61 mg g^{-1}, much higher than that of the calcined Mg/Al layered supramolecular compound (Mg/Al-CLDH) (199.41 mg g^{-1}). The main reason for this high saturated adsorption capacity of the material was that Cr(VI) was reduced to Cr(III) by Fe(II) in the LDH host layer, and then, Cr(III) combined with OH^- to yield $Cr(OH)_3$. The sorption kinetics of Mg/Al/Fe-CLDH for Cr(VI) were appropriately described by the pseudo-second order, Elovich, and intraparticle diffusion models. Furthermore, Mg/Al/Fe-CLDH exhibited excellent regenerative property. Hence, Mg/Al/Fe-LDH could be potentially used as a structured adsorbent for Cr(VI) in laboratory wastewater.

Received 25th April 2017
Accepted 21st June 2017

DOI: 10.1039/c7ra04646d

rsc.li/rsc-advances

1. Introduction

Wastewater mainly derived from all kinds of laboratories including those in the research, education, industrial, and agricultural institutions has not attracted enough attention. In these laboratories, various physical and chemical tests are often conducted on a day-to-day basis that lead to unknown and changing effluents. Laboratory wastewater containing heavy metals is particularly hazardous and will give rise to serious environmental problems. Cr(VI) is a common contaminant in laboratory wastewater, which has a carcinogenic and mutagenic effect on humans.[1] Long-term exposure to Cr(VI) will increase the risk of bladder, liver, kidney, and skin cancers.[2,3] The traditional methods of wastewater treatment include reduction precipitation, biological process, ion-exchange, sorption, membrane filtration, and so on.[4–7] The sorption method is one of the frequently-used methods for the removal of Cr(VI) from wastewater. Hence, it is necessary to achieve a high sorption capacity and low-cost material for the treatment of Cr(VI) in laboratory wastewater.

There are different kinds of adsorbents for the removal of Cr(VI). Layered double hydroxides (LDH), also known as supramolecular compounds, are a good anion-exchanging materials with large surface areas, homogeneous inner dispersion of the elements, and calcination-reconstruction.[8] They constitute a large family of two-dimensional (2D) anionic clays consisting of positively charged host layers and exchangeable interlayer anions.[9] The adsorption property of LDH depends on the M(II)/M(III) molar ratio, guest anions, and layer structure.[10] They have been widely used as adsorbents for the removal of chromium.[11–14] He S. *et al.* investigated a Mg–Al layered double hydroxide framework for the removal of Cr(VI) and found that the sorption capacities (q_{max}) of the LDH framework reached 27.8 mg g^{-1}.[15] Wang W. W. *et al.* synthesized LDH comprising Mg/Al, Ni/Al, and Zn/Al with a molar ratio of 3 : 1 *via* a facile hydrothermal route, and Zn/Al-LDH exhibited an excellent sorption capacity (68.07 mg g^{-1}) for Cr(VI).[16] There are also other reports on the removal of Cr(VI) using LDH in water treatment.[17–19] However, the application of LDH showed the following drawbacks: lower adsorption capability and poor regeneration capacity. From this point of view, modified LDH as an excellent adsorbent is an effective solution for these problems. Tomohito K. *et al.* prepared uncalcined chloride 6Mg/2Fe/2Al layered double hydroxide to remove Cr(VI) and improved the adsorption capability up to 650 mg g^{-1} *via* anion-exchange and oxidation–reduction.[20]

[a]*College of Materials and Chemistry & Chemical Engineering, Mineral Resources Chemistry Key Laboratory of Sichuan Higher Education Institutions, Chengdu University of Technology, Chengdu 610059, China. E-mail: zhuxiaping@cdut.edu.cn*
[b]*Jiangsu Institute of Zoneco Soil Co., Ltd., Yixing 214200, China*

We studied the fabrication of a carbonate Mg/Al/Fe layered supramolecular compound (Mg/Al/Fe-LDH) using the co-precipitation method and applied the calcined Mg/Al/Fe layered supramolecular compound (Mg/Al/Fe-CLDH) to remove Cr(VI) in laboratory wastewater. The preparation process of Mg/Al/Fe-LDH was studied in-depth based on the removal rate of Cr(VI). The adsorption process, adsorption selectivity, saturation adsorption capacity, and adsorption mechanism of Mg/Al/Fe-CLDH to Cr(VI) were investigated. The study might lead to the further development of a cost-effective and recyclable adsorbent for the removal of Cr(VI) in laboratory wastewater.

2. Experimental

2.1. Materials

$Mg(NO_3)_2 \cdot 6H_2O$, $Al(NO_3)_3 \cdot 9H_2O$, $FeSO_4 \cdot 7H_2O$, $K_2Cr_2O_7$, $HNO_3 \cdot NaOH$, Na_2CO_3, acetone, and diphenylcarbazide were obtained from the Kelong Chemical Reagent Factory (Chengdu, China). All chemicals used in the experiments were of analytical grade and used as received without any further treatment. The Cr(VI) solutions were prepared by dissolving K_2CrO_4 in distilled water.

2.2. Preparation of the adsorption materials

2.2.1. Preparation of Mg/Al/Fe-LDH. Mg/Al/Fe-LDH was prepared by the co-precipitation method. Herein, 0.01 mol $Mg(NO_3)_2 \cdot 6H_2O$, 0.004 mol $Al(NO_3)_3 \cdot 9H_2O$, and 0.002 mol $FeSO_4 \cdot 7H_2O$ were dissolved in 250 mL of distilled water. Mg/Al/Fe mixed solution was then added dropwise to 200 mL 0.04 mol L^{-1} Na_2CO_3 solution under stirring at 25 °C. The solution pH was adjusted to 10 *via* the addition of 1 mol L^{-1} NaOH solution. N_2 was bubbled into the reaction system for deoxidation throughout the process of preparation. After the reaction terminated, the resulting precipitate was aged at 80 °C for 24 h. The product was filtered, washed to remove sodium ions, and dried at 40 °C in a vacuum drying oven. The Mg/Al/Fe-CLDH was obtained by calcination at 400 °C for 2 h in a pipe furnace under a nitrogen atmosphere.

2.2.2. Preparation of Mg/Al-LDH. Herein, 0.012 mol $Mg(NO_3)_2 \cdot 6H_2O$ and 0.004 mol $Al(NO_3)_3 \cdot 9H_2O$ were dissolved in 250 mL water. Mg/Al-LDH was prepared according to the preparation method of Mg/Al/Fe-LDH. During this period, N_2 was not bubbled into the reaction system, and the product was dried in an air dry oven. Mg/Al-CLDH was obtained by calcination at 400 °C for 2 h in a muffle furnace.

2.3. Adsorption tests

Typically, 0.100 g of Mg/Al/Fe-CLDH was added to 25 mL of simulated laboratory wastewater containing 50 mg L^{-1} of Cr(VI). The mixture was oscillated using a thermostatic shaker for 100 min at room temperature. The solution pH was adjusted between 9 and 10 using 0.1 mol L^{-1} HNO_3 or NaOH solution. The sample was separated from the solution *via* centrifugation at 4000 rpm, and the Cr(VI) concentration in the aqueous solution was determined by diphenylcarbazide spectrophotometry.[21]

2.4. Desorption and regeneration cycles

The Cr(VI)-loaded Mg/Al/Fe-LDH was added to 100 mL of 0.01 mol L^{-1} Na_2CO_3 solution. The shaking desorption lasted for 30 min at room temperature and was repeated a few times until the upper supernatant was colorless. Mg/Al/Fe-LDH after regeneration was dried in an air dry oven and then calcined in a muffle furnace at 400 °C for 2 h. The regenerative test was repeated five times.

2.5. Characterization

X-ray diffraction pattern was obtained using a DX-2700 diffractometer with CuKα radiation at 40 kV and 30 mA. The scan was acquired between 5° and 70° (2θ) with a step size of 0.06°. Infrared spectrum was obtained using a TENSOR27 Fourier transform infrared spectrometer in the range of 400–4000 cm^{-1} employing the KBr dilution technique (1.5%, w/w). Thermogravimetric analysis was conducted using a NETZSCH STA409PC Luxx simultaneous thermal gravimetric analyzer. The curve was obtained in the temperature range from 30 to 700 °C at a scanning rate of 10 °C min^{-1} under a high-purity flowing nitrogen atmosphere (50 cm^3 min^{-1}). The Brunauer–Emmett–Teller (BET) surface area was measured using a VacPrep 06 micromeritics surface area analyzer at 77 K *via* an adsorption apparatus. Scanning electron microscopy was performed using a ZEISS S-4800 emission-scanning electron microscope scanned at an acceleration voltage of 10 kV. Zeta potential analysis was conducted using a Malvern Zetasizer Nano ZS 90 instrument at 25 °C. X-ray photoelectron spectroscopy was performed using a VG Escalab 250 spectrometer equipped with an Al anode (Al-Kα = 1486.7 eV).

3. Results and discussion

3.1. Preparation process of Mg/Al/Fe-LDH

Fig. 1a shows the effect of the M(II)/M(III) molar ratio on Mg/Al/Fe-CLDH for the removal rate of Cr(VI) *via* variation in the amount of Al(III). In this case, M(II) and M(III) represented divalent metal ions and trivalent metal ions, respectively. The removal rate first increased and then decreased with the increase in the M(II)/M(III) molar ratio. At lower molar ratios, Al(III) had a greater chance to form an $Al(OH)_3$-like structure. The LDH crystal was not well developed, which caused the low removal rate. With the increase in the molar ratio, the removal rate gradually increased. Al(III) distributed well in the brucite-like layers that developed the LDH phase with Al–OH stabilized by the adjacent M(II)–OH in the structure.[22] At higher molar ratios, the number of positive charges in the laminate gradually reduced and the removal rate began to decrease. The removal rate was maximum when the molar ratio was 3 : 1. Therefore, the M(II)/M(III) molar ratio of 3 : 1 was chosen for further experiments.

The effect of the Mg(II)/Fe(II) molar ratio on the removal rate of Cr(VI) by Mg/Al/Fe-CLDH is shown in Fig. 1b. The removal rate

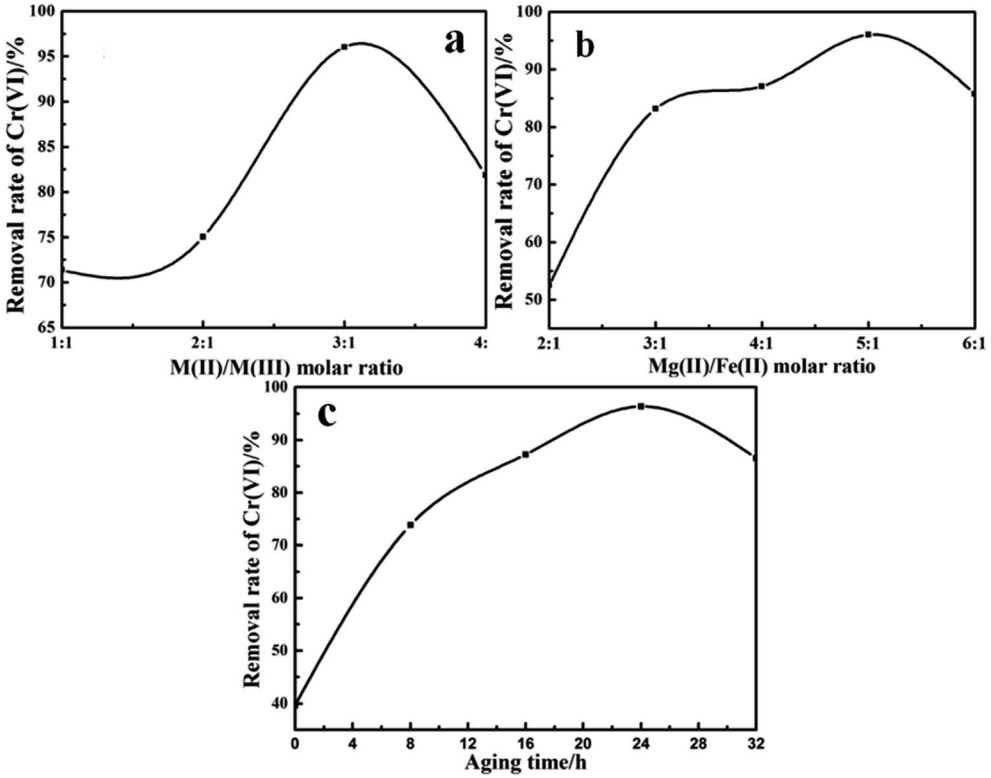

Fig. 1 Effect of M(II)/M(III) molar ratio (a), Mg(II)/Fe(II) molar ratio (b), and aging time (c) on the removal rate of Cr(VI).

increased in the molar ratio range from 2 : 1 to 5 : 1 and then decreased when the molar ratio was higher than 5 : 1. At lower molar ratios, the Fe(II) content was too high and the LDH crystal was not fabricated well. At higher molar ratios, the reduction of Fe(II) gradually weakened; thus, the removal rate of Cr(VI) began to decrease. Taking the abovementioned factors into account, a Mg(II)/Fe(II) molar ratio of 5 : 1 was confirmed.

During the preparation process, the aging time had a significant effect on the LDH formation further affected the removal efficiency of Cr(VI). The experimental results are shown in Fig. 1c. The removal rate of Cr(VI) continuously increased with the increase in the aging time. The resulting precipitate was aged for 24 h. For the crystalline precipitate, aging has two vital functions as follows. The first function is the removal of impurities in the precipitate and the second function is that *via* aging, the crystal grain size slowly becomes large and homogeneous. For a relatively long aging time, Fe(II) may be oxidized to Fe(III), which results in the reduction of the removal rate. Therefore, 24 h was selected as the optimum aging time.

3.2. Characterization of LDH and CLDH

3.2.1. X-ray diffraction patterns. Fig. 2 shows the X-ray diffraction patterns of Mg/Al-LDH, Mg/Al/Fe-LDH, Mg/Al/Fe-CLDH, and Cr(VI)-loaded Mg/Al/Fe-CLDH. The XRD patterns of Mg/Al/Fe-LDH (Fig. 2b) showed diffraction peaks, which agreed well with the characteristic peaks of Mg/Al-LDH (Fig. 2a). These diffraction lines could be assigned to the (003), (006), (009), (015), (012), (110), and (113) planes.[23,24] Mg/Al/Fe-LDH was of higher purity and crystallinity because of the intense and sharp diffraction peaks. The diffraction peaks of (003) and (006) were especially strong at low 2θ values, whereas other peaks had relatively weak intensities at high 2θ values, showing that the crystal grew along a certain axis. The basal spacing calculated from d_{003} was 0.753 nm, close to the value (0.749 nm) reported for carbonate Mg/Al-LDH. The XRD pattern of Mg/Al/Fe-CLDH (Fig. 2c) showed that the characteristic peaks of Mg/Al/Fe-LDH disappeared and two broad peaks were observed, corresponding to the (200) and (220) planes. The appearance of broad

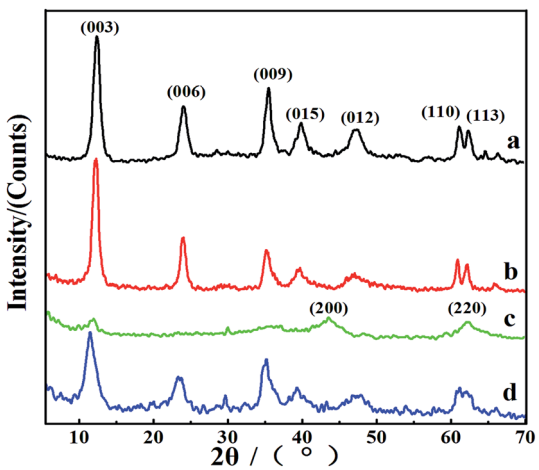

Fig. 2 X-ray diffraction patterns of Mg/Al-LDH (a), Mg/Al/Fe-LDH (b), Mg/Al/Fe-CLDH (c) and Cr-loaded Mg/Al/Fe-LDH (d).

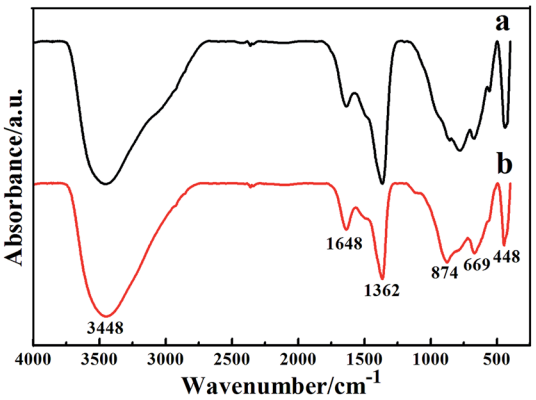

Fig. 3 Infrared spectra of Mg/Al/Fe-LDH (a) and Cr-loaded Mg/Al/Fe-LDH (b).

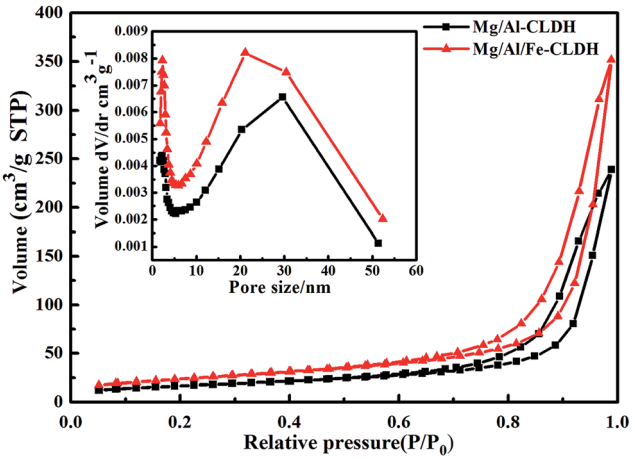

Fig. 4 N_2 adsorption–desorption and pore size of distribution curves of Mg/Al/Fe-CLDH and Mg/Al-CLDH.

peaks was attributed to the formation of Mg, Al, and Fe mixed oxides, indicating that the layered structure of Mg/Al/Fe-LDH was destroyed at 400 °C. After adsorption of Cr(VI) from aqueous solution, the Cr-loaded Mg/Al/Fe-LDH (Fig. 2d) regained the characteristic reflections of Mg/Al/Fe-LDH. However, the peaks were broadened and their intensities decreased as compared to those of Mg/Al/Fe-LDH, indicating the reduction in crystallinity after rehydration.[25] Furthermore, the (003) plane moved in the direction of lower 2θ values and the layer spacing increased to 0.813 nm, and Cr(VI) was successfully incorporated into the interlayer of the material. Magnesium, aluminum, and iron mixture hydroxide contributed to the formation of the laminate of the supramolecular material. The interlayer anions were H_2O, OH^-, CO_3^{2-}, and CrO_4^{2-}. The negatively charged anions were connected to the laminate depending on the electrostatic attraction, hydrogen bonding, and so on, which would form a three-dimensional structure. It was automatically combined into an ordered, organized polymerization system with a supramolecular structure *via* an intermolecular force.

3.2.2. Infrared spectra. The FT-IR spectra are shown in Fig. 3. The absorption band appeared at 3448 cm^{-1} because of the O–H stretching vibration of the interlayer water molecules.[26] There was also a vibration band at 1646 cm^{-1}, corresponding to the bending vibration of O–H. Furthermore, the vibration band at 1362 cm^{-1} was ascribed to the interlayer CO_3^{2-} anions. The sharp bands around 669 and 448 cm^{-1} were caused by various lattice vibrations associated with the metal hydroxide sheets.[27] After adsorption of Cr(VI), a new band was observed at 874 cm^{-1} in Fig. 3b. This could be attributed to the stretching vibration of Cr–O. Cr(VI) was successfully absorbed on Mg/Al/Fe-CLDH, which was in good agreement with the XRD results.

3.2.3. N_2 adsorption–desorption and pore size distribution curves. The porous structures of Mg/Al/Fe-CLDH and Mg/Al-CLDH were analyzed by N_2 adsorption–desorption curves and pore size distribution curves. As shown in Fig. 4, the adsorption–desorption isotherms of CLDH had a shape similar to that of the characteristic of type IV isotherms.[28] The hysteresis loops were of type H3, ascribed to the slit-shaped pores with a non-uniform size and shape, which were created by the collapse of LDH calcined at 400 °C.[29] According to the determined pore diameter (peak pore at *ca.* 2–20 nm), CLDH could be classified as mesoporous solids. However, some differences still existed with regard the size of the hysteresis loops of different samples. The surface areas of Mg/Al-CLDH and Mg/Al/Fe-CLDH were 68.6 $m^2\ g^{-1}$ and 85.6 $m^2\ g^{-1}$, respectively. Mg/Al/Fe-CLDH with the most narrow hysteresis loop had bigger surface area and more micropores and mesopores. The bigger surface area was crucial for the adsorption capacity because of more active sites.

3.2.4. SEM images. To further analyze the microstructural features of the material, SEM images of Mg/Al/Fe-LDH and Mg/Al-LDH were studied. As seen from Fig. 5, Mg/Al/Fe-LDH and Mg/Al-LDH exhibited mainly platelet structures and perfect

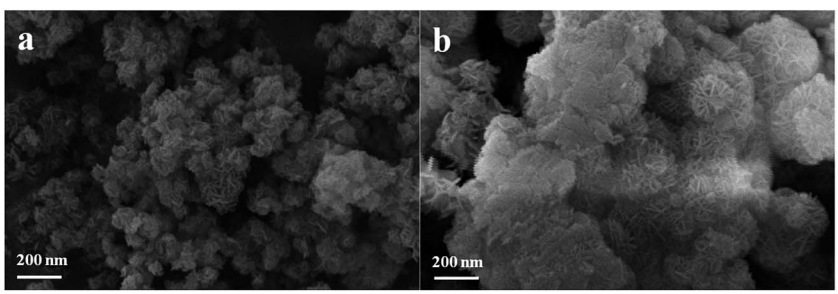

Fig. 5 SEM images of Mg/Al/Fe-LDH (a) and Mg/Al-LDH (b).

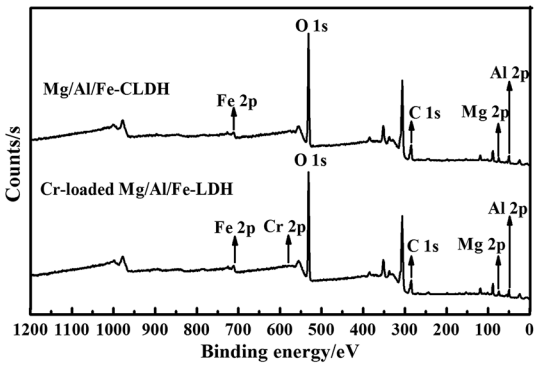

Fig. 6 Wide scan XPS spectra of Mg/Al/Fe-CLDH and Cr-loaded Mg/Al/Fe-LDH.

morphologies because of the sufficient aging time. Compared to that of Mg/Al-LDH, the particle size of Mg/Al/Fe-LDH was smaller and the surface of Mg/Al/Fe-LDH was looser, which explained its better adsorption property.

3.2.5. XPS spectra. The wide scan XPS spectra of Mg/Al/Fe-CLDH and Cr-loaded Mg/Al/Fe-LDH are shown in Fig. 6. As can be seen, the peaks for Mg 2p, Fe 2p, Al 2p, C 1s, and O 1s were observed in the wide scan XPS spectra of Mg/Al/Fe-CLDH and Cr-loaded Mg/Al/Fe-LDH.[30] However, compared to the case of Mg/Al/Fe-CLDH, new peaks for Cr 2p were detected in the Cr-loaded Mg/Al/Fe-LDH, which further verified the adsorption of Cr(VI). The high resolution XPS spectra of Fe 2p and Cr 2p were obtained to determine the reaction between Cr(VI) and Mg/Al/Fe-CLDH, as shown in Fig. 7. The relative value of the Fe(III)/Fe(II) peak areas (2.48) in the Cr-loaded Mg/Al/Fe-LDH increased as compared to the values obtained before adsorption (0.75), as shown in Fig. 7a and b.[31] These results confirmed that the oxidation of Fe(II) to Fe(III) took place during adsorption. In the spectrum corresponding to the Cr 2p region in Fig. 7c, the peaks at 577.4 eV indicated the existence of Cr(III) species, whereas the peak at 586.5 eV was assigned to Cr(VI).[30] These results confirmed the abovementioned hypothesis that the laminate Fe(II) in Mg/Al/Fe-CLDH promoted the transformation of Cr(VI) into Cr(III). Moreover, these results confirmed that the removal mechanism involved combined adsorption–reduction processes.

3.3. Removal process of Cr(VI) on Mg/Al/Fe-CLDH

To determine the equilibration time of Cr(VI) adsorption and investigate the adsorption kinetics, the effect of vibration time on the removal rate of Cr(VI) was studied. As can be seen from Fig. 8a, the removal rate of Cr(VI) on Mg/Al/Fe-CLDH initially increased and then slowed down with an increase in the contact time. After vibrating for about 100 min, the removal rate of Cr(VI) became almost constant, and the equilibrium adsorption removal rate for Cr(VI) was 94.50%. Compared to other reported adsorbents, Mg/Al/Fe-CLDH showed faster adsorption.[15,32,33] This fast adsorption could be attributed to the larger surface area and different removal mechanisms, including electrostatic interaction, calcination-reconstruction, and oxidation–reduction, of Cr(VI).[20]

The pH-dependent single-component is one of the most important parameters affecting the removal of Cr(VI). Fig. 8b shows the effect of pH value on Cr(VI) removal depending on

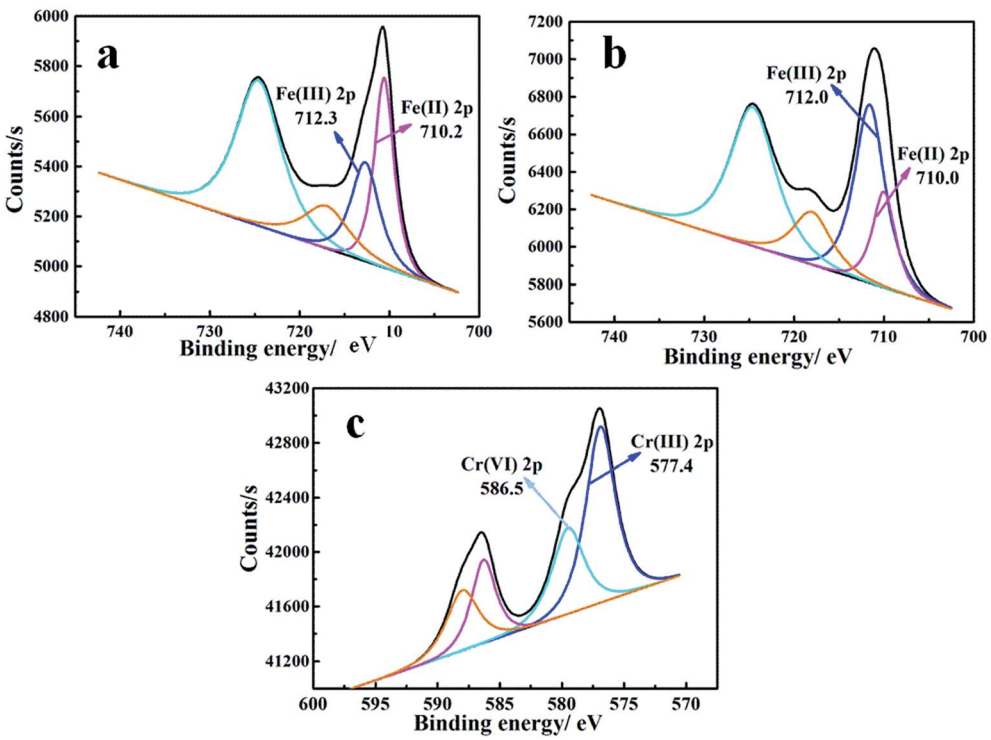

Fig. 7 Narrow scan Fe 2p of Mg/Al/Fe-CLDH (a), Fe 2p of Cr-loaded Mg/Al/Fe-LDH (b), and Cr 2p of Cr-loaded Mg/Al/Fe-LDH (c).

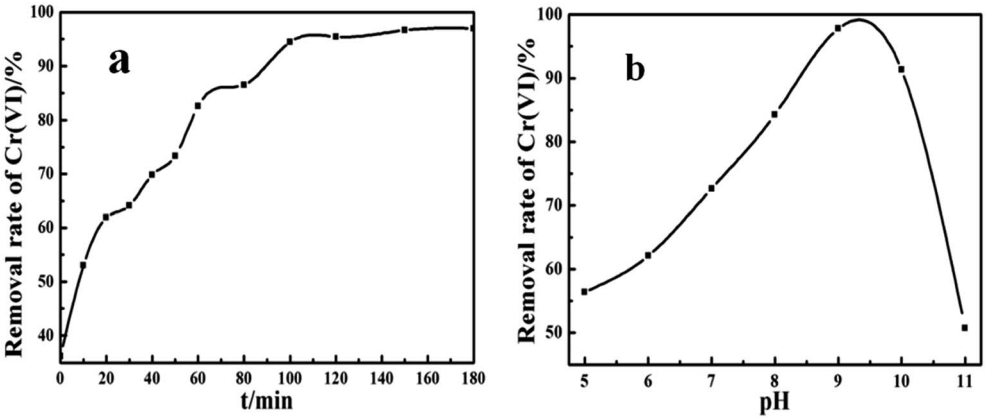

Fig. 8 Effect of vibration time (a) and pH value (b) on the removal rate of Cr(VI).

Mg/Al/Fe-CLDH. With the initial pH ranging from 5 to 11, the removal rate of Cr(VI) first increased and then decreased. The removal rate attained a maximum value at a pH between 9 and 10. When the pH was lower, Mg/Al/Fe-CLDH could be partly dissolved. The pH_{pzc} of CLDH was 11. When the pH was below the pH_{pzc} of CLDH, the adsorption of hexavalent chromium anions was facilitated. Moreover, Mg/Al/Fe-CLDH could be better restored to the original layered structure for the adsorption of anions. At a higher pH (>10), the high concentration of OH^- could reduce the Cr(VI) uptake because of its high affinity to CLDH.[34] Therefore, a pH value between 9 and 10 was an ideal parameter for this study.

3.4. Comparative study of Mg/Al/Fe-CLDH and Mg/Al-CLDH on the removal of Cr(VI)

Laboratory wastewater often contains various ions, which strongly compete with Cr(VI) adsorption for the active adsorption sites on the LDH. Therefore, the adsorption selectivity was studied by adding a KNO_3 solution. As shown in Fig. 9a, the concentration of NO_3^- increased from 0.02 to 0.24 mol L^{-1}, with the removal rate of Cr(VI) trending downward. In general, the forces of adsorption of Cr(VI) on CLDH were unselective and weak. However, the adsorption of Cr(VI) on Mg/Al/Fe-CLDH included a selective and strong oxidation–reduction. Hence, as a conventional layered supramolecular compound, Mg/Al/Fe-CLDH had better adsorption selectivity as compared to Mg/Al-CLDH, especially when the concentration of NO_3^- was less than 0.12 mol L^{-1}.

For achieving the saturated adsorption capacity of Cr(VI) by Mg/Al/Fe-CLDH and Mg/Al-CLDH, the initial concentration of Cr(VI) was increased from 50 to 6000 mg L^{-1}. Fig. 9b shows the adsorption isotherm of Cr(VI) on CLDH. The equilibrium adsorption amount rapidly increased with the increase in the initial concentration and then reached a plateau. The saturated adsorption capacity of Mg/Al/Fe-CLDH reached 725.61 mg g^{-1} and that of Mg/Al-CLDH was only 199.41 mg g^{-1}. The adsorption capacity of Mg/Al/Fe-CLDH was significantly improved. Table 1 lists a the comparison of the maximum adsorption capacity of Cr(VI) on different hydrotalcite materials reported under the optimal process condition in the literature. The Mg/Al/Fe-CLDH prepared in this study showed relatively large adsorption capacity as compared to those reported in the previous studies. In general, LDH can remove Cr(VI) in wastewater *via* electrostatic attraction on the surface and interlayer of materials. The CLDH can also rebuild the initial layered structure by adsorbing Cr(VI). The memory effect has a stronger ability for the removal of Cr(VI) than that of ion-exchange. In the study, we prepared Mg/Al/Fe-CLDH by doping with Fe(II). Based on the abovementioned facts, Cr(VI) was reduced to Cr(III) by Fe(II) in the LDH host layer, and then, Cr(III) was removed *via* the formation of $Cr(OH)_3$.

The regenerative property is an important indicator in the evaluation of sorbents. The regenerative tests of Mg/Al/Fe-CLDH and Mg/Al-CLDH were repeated five times under uniform experimental conditions as abovementioned in Sections 2.3 and 2.4. The results for each cycle are shown in Fig. 9c. Compared to that on Mg/Al-CLDH, the removal rate of Cr(VI) on Mg/Al/Fe-CLDH was still more than 97% at the last regeneration, and it had better regenerative property. The recovered Cr(VI) can be used as a valuable chemical raw material; this is a process of turning waste into treasure.

3.5. Treatment of integrative laboratory wastewater

To further confirm the practical application of Mg/Al/Fe-CLDH, the actual integrative laboratory wastewater containing Cr(VI) was treated, which was derived from a comprehensive laboratory. The wastewater was yellow-green, slightly acidic, and contained 226.13 mg L^{-1} Cr(VI). The result obtained using the optimized process is shown in Table 2. The remaining Cr(VI) concentration was less than 0.5 mg L^{-1} after five processes, in line with the national sewage comprehensive emission standard (GB8978-1996).[38] The laboratory wastewater can be directly discharged after the treatment process. This result indicates a good practical application of Mg/Al/Fe-CLDH in laboratory wastewater treatment.

3.6. Adsorption kinetics

Herein, four adsorption kinetic models, *i.e.* pseudo-first order (eqn (1)), pseudo-second order (eqn (2)), Elovich (eqn (3)), and

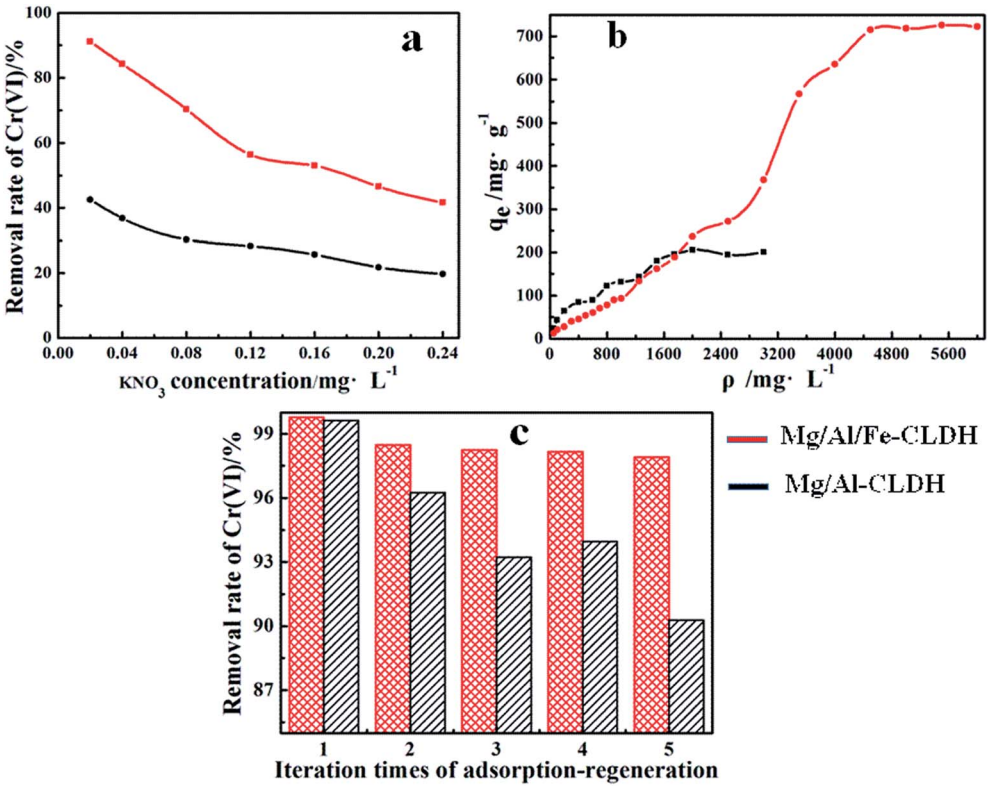

Fig. 9 Adsorption selectivity (a), saturated adsorption capacity (b), and regenerative property (c) of Mg/Al/Fe-CLDH and Mg/Al-CLDH.

intraparticle diffusion model (eqn (4)), were used to describe the sorption mechanism of Cr(VI) on Mg/Al/Fe-CLDH.[39,40] These models are generally expressed as follows.

$$\ln(q_e - q_t) = \ln q_e - k_1 t \quad (1)$$

Table 1 Comparison between the maximum adsorption capacities of Cr(VI) on other hydrotalcite materials

Adsorbents	q_{max} (mg g^{-1})	References
Zn/Al–CO_3-LDH	68.07	16
Calcined graphene–Mg/Al-LDH	172.55	17
Ca/Al–Cl-LDH	42.92	18
6Mg2Fe2Al–Cl-LDH	650	20
Oriented Mg/Al–NO_3-LDH	79.4	32
Mg/Al-LDH/ESM	27.9	35
Li/Al-LDH	177	36
Calcined Mg/Al–CO_3-LDH	120	37
Mg/Al/Fe-CLDH	725.81	Present work
Mg/Al-CLDH	199.41	Present work

Table 2 Treatment result of the wastewater laboratory using Mg/Al/Fe-CLDH

Number of times	1	2	3	4	5
Remaining of Cr(VI) concentration (mg L^{-1})	188.02	102.79	48.56	8.47	0.16

$$\frac{t}{q_t} = \frac{1}{k_2 q_e^2} + \frac{t}{q_e} \quad (2)$$

$$q_t = \frac{1}{\tau}\ln(k_3\tau) + \frac{1}{\tau}\ln t \quad (3)$$

$$q_t = k_4 t^{0.5} + b \quad (4)$$

where q_e and q_t are the adsorptive amounts of Cr(VI) (mg g^{-1}) at equilibrium and at time t (min), respectively. The values of k_1 (min^{-1}), k_2 (g mg^{-1} min^{-1}), k_3 (mg g^{-1} min$^{-0.5}$), and k_4 (g mg^{-1} min^{-1}) are the adsorption rate constants for the pseudo-first order, pseudo-second order, intraparticle diffusion, and Elovich models. τ and b are constants.

The obtained results are shown in Fig. 10 and Table 3. The pseudo-first order model resulted in lower R^2 values, and the $q_{e,cal}$ was far from the experimental value ($q_{e,exp}$ = 12.06 mg g^{-1}). Usually, the pseudo-first order model was the best fit for the initial period of adsorption. Fig. 8a shows the suitability of the pseudo-second-order kinetic model for the complete evaluation of the adsorption process, which shows a straight line with a high correlation coefficient (R^2 = 1.0000). The $q_{e,cal}$ based on the pseudo-second order model was generally in good agreement with $q_{e,exp}$, which suggested that the sorption process of Cr(VI) involved a chemisorption process. It could also be seen that the Elovich model better fitted the entire adsorption process, suggesting that the material was heterogeneous in energy. The adsorption of Cr(VI) was first a rapid and then a slow heterogeneous diffusion process,

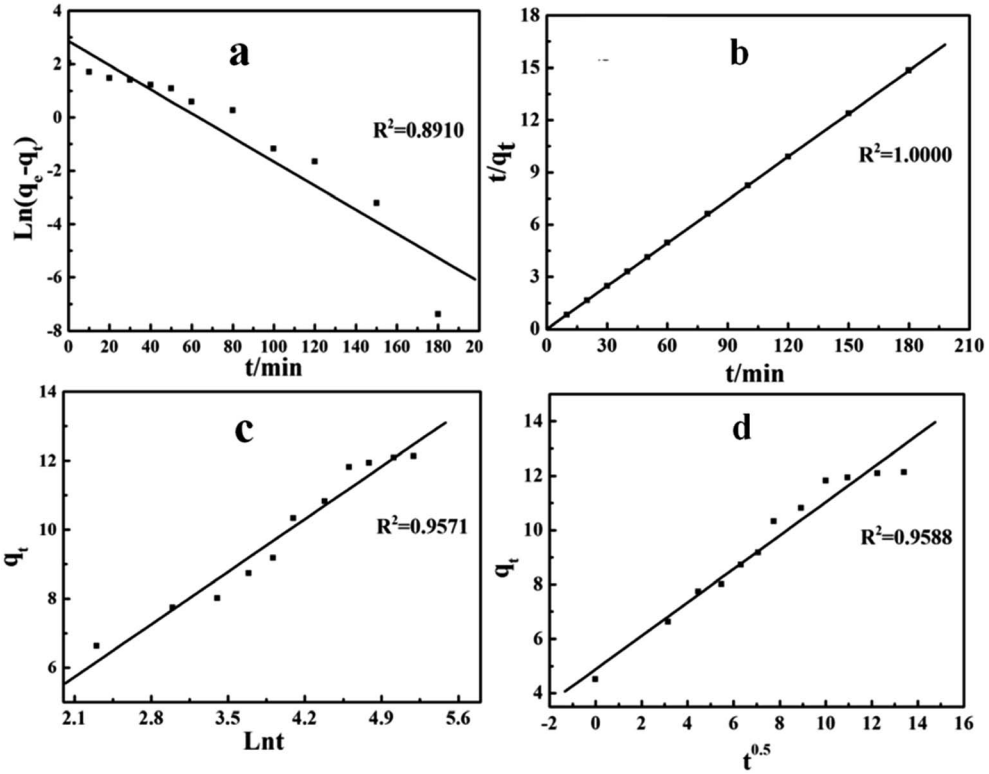

Fig. 10 Fitting of the experimental results by pseudo-first order (a), pseudo-second order (b), Elovich (c), and intraparticle diffusion model (d).

which was consistent with the trend of the dynamic curve (Fig. 8a). The intraparticle diffusion process was controlled by the diffusion of ions within the adsorbent. The intraparticle diffusion model also fitted well the adsorption process. The mechanism of transfer of Cr(VI) to the material included diffusion through a fluid film around the adsorbent particle and pores to the internal adsorption sites. Initially, the concentration gradient between the film and the solid surface was large, and the transfer of Cr(VI) in the absorbent surface was faster. As the time increased, intraparticle diffusion became predominant, and Cr(VI) took more time to transfer from the surface of Mg/Al/Fe-CLDH to the internal adsorption sites through the pores. However, the presence of b in the obtained intraparticle diffusion model indicated that the boundary layer effect could be another rate limiting factor.[41]

Table 3 Kinetics parameters for Cr(VI) adsorption by Mg/Al/Fe-CLDH

Kinetic model	Parameters	Numerical value	R^2
Pseudo-first order model	k_1	0.045	0.8910
	$q_{e,cal}$	17.35	
Pseudo-second order model	k_2	—	1.0000
	$q_{e,cal}$	12.12	
Elovich model	k_3	3.69	0.9571
	τ	0.46	
Intraparticle diffusion model	k_4	0.62	0.9588
	b	4.89	

3.7. Possible removal mechanism of Cr(VI)

According to the abovementioned experimental results, the mechanism *via* which the Mg/Al/Fe layered compound removed Cr(VI) in laboratory wastewater was proposed, as shown in Scheme 1. According to the co-precipitation method, Mg/Al/Fe-LDH was prepared in a nitrogen atmosphere using a mixed metal solution, which consisted of magnesium, aluminum, and iron. Magnesium, aluminum, and iron metal hydroxide formed the laminate of LDH, and there were some anions and water molecules in the interlayer of LDH. After calcination under a nitrogen atmosphere, CO_3^{2-}, OH^-, and H_2O were removed and the interlayer structure of Mg/Al/Fe-LDH was destroyed, but the material still maintained the original laminate structure. When Mg/Al/Fe-CLDH was added to the laboratory wastewater containing Cr(VI), part of Cr(VI) was removed by the electrostatic attraction between Cr(VI) and the outer layer particle of the

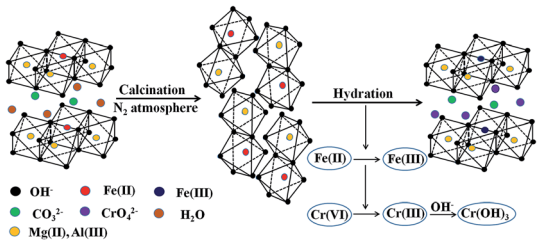

Scheme 1 Schematic for Cr(VI) treatment in laboratory wastewater using the Mg/Al/Fe layered compound.

material surface. Cr(VI) selectively intercalated into the interlayer of Mg/Al/Fe-CLDH to neutralize the positive charge of the laminate *via* a memory effect. Moreover, Cr(VI) was reduced to Cr(III) *via* the oxidation of Fe(II) in the LDH host layer, and then, Cr(III) was combined with OH^- to yield $Cr(OH)_3$. Hence, Mg/Al/Fe-LDH *via* doping with Fe(II) could effectively treat Cr(VI) pollution in laboratory wastewater.

4. Conclusions

In summary, Mg/Al/Fe-LDH was successfully prepared by the co-precipitation method. The magnesium, aluminum, and iron mixture hydroxide contributed to the formation of the laminate of the supramolecular material. The interlayer anions were connected to the laminate depending on the electrostatic attraction, hydrogen bonding, and so on, which would form an ordered, organized three-dimensional supramolecular structure. Compared to Mg/Al-CLDH, Mg/Al/Fe-CLDH exhibited higher adsorption efficiency to Cr(VI) in laboratory wastewater. The first reason was because of the electrostatic attraction between Cr(VI) and the outer layer particle of the material surface. The second reason was that Cr(VI) selectively intercalated into the interlayer of Mg/Al/Fe-CLDH *via* a memory effect. The last reason was that Cr(VI) was reduced to Cr(III) by Fe(II) in the LDH host layer, and then, Cr(III) was combined with OH^- to yield $Cr(OH)_3$. The Mg/Al/Fe-LDH could be regenerated and used up to five times. It is expected that Mg/Al/Fe-CLDH can be potentially used as an efficient and recyclable adsorbent in laboratory wastewater treatment.

Acknowledgements

This work was supported by the financial support received from the Natural Science Foundation of the Education Department of Sichuan Province (15ZA0071) and the Science and Technology Department of Sichuan Province (2015GZ0243).

Notes and references

1 I. Eichlerová, L. Homolka, O. Benada, O. Kofroňová, T. Hubálek and F. Nerud, *Chemosphere*, 2007, **69**, 795–802.
2 X. J. Wang, X. P. Zhu, L. M. Lan and H. B. Zuo, *RSC Adv.*, 2016, **6**, 85595–85602.
3 M. Costa, *Toxicol. Appl. Pharmacol.*, 2003, **188**(1), 1–5.
4 X. P. Zhu, J. R. Ni and P. Lai, *Water Res.*, 2009, **43**(17), 4347–4355.
5 N. Dizge, E. Demirbas and M. Kobya, *J. Hazard. Mater.*, 2009, **66**(2–3), 1367–1376.
6 M. X. Zhu, Y. P. Li, M. X. Xie and H. Z. Xin, *J. Hazard. Mater.*, 2005, **120**(1), 163–171.
7 S. H. Jin, S. Liang, W. G. Zhong and L. J. Wan, *Adv. Mater.*, 2008, **20**(15), 2977–2982.
8 S. L. Wang, C. H. Liu, M. Kuang and P. N. Chiang, *Appl. Clay Sci.*, 2009, **43**(1), 79–85.
9 Z. P. Xu, J. Zhang, M. O. Adebajo, H. Zhang and C. H. Zhou, *Appl. Clay Sci.*, 2011, **53**(2), 139–150.
10 J. Zhang, Y. F. Xu and G. R. Qian, *J. Phys. Chem.*, 2010, **114**(24), 10768–10774.
11 Q. Zhao, Z. Chang, X. Lei and X. M. Sun, *Ind. Eng. Chem. Res.*, 2011, **50**(17), 10253–10258.
12 L. G. Yan, Y. Y. Xu, H. Q. Yu, X. D. Xin and B. Du, *J. Hazard. Mater.*, 2010, **179**, 244–250.
13 M. Dadwhal, M. Sahimi and T. T. Theodore, *Ind. Eng. Chem. Res.*, 2011, **50**(4), 2220–2226.
14 S. Mandal, S. Mayadevi and B. D. Kulkarni, *Ind. Eng. Chem. Res.*, 2009, **48**(17), 7893–7898.
15 S. He, Y. F. Zhao, M. Wei, D. G. Evans and X. Duan, *Ind. Eng. Chem. Res.*, 2012, **51**(1), 285–291.
16 W. W. Wang, J. B. Zhou, G. Achari, J. G. Yu and W. Q. Cai, *Colloids Surf., A*, 2014, **457**, 33–40.
17 X. Y. Yuan, Y. F. Wang, J. Wang, C. Zhou, Q. Tang and X. B. Rao, *Chem. Eng. J.*, 2013, **221**, 204–213.
18 J. Zhang, Y. Li, J. Z. Zhou, D. Chen and G. G. Qian, *J. Hazard. Mater.*, 2012, **205**, 111–117.
19 E. R. Ramírez, N. L. G. Ortega, C. A. C. Soto and M. T. Gutiérrez, *J. Hazard. Mater.*, 2009, **172**(2–3), 1527–1531.
20 K. Tomohito, K. Eisuke and Y. Toshiaki, *Sep. Purif. Technol.*, 2014, **122**, 12–16.
21 F. S. Wei, *Water and Exhausted Water Monitoring Analysis Methods*, China Environmental Science Press, Beijing, 3rd edn, 1998, pp. 157–159.
22 J. Z. Zhou, Y. Y. Wu, C. Liu, A. Orpe, Q. Liu, Z. P. Xu, G. R. Qian and S. Z. Qiao, *Environ. Sci. Technol.*, 2010, **44**, 8884–8890.
23 A. R. Auxilio, P. C. Andrews and P. C. Junk, *Dyes Pigm.*, 2009, **81**(2), 103–112.
24 D. Carriazo, M. D. Arco, C. Martín and V. Rives, *Appl. Clay Sci.*, 2007, **37**(3–4), 231–239.
25 P. Cai, H. Zheng, C. Wang, H. Ma, J. Hu, Y. Pu and P. Liang, *J. Hazard. Mater.*, 2012, **213**, 100–108.
26 S. Mallakpour, F. Tirgir and M. R. Sabzalian, *Amino Acids*, 2011, **40**(2), 611–621.
27 P. K. Trowski, D. Sułkowska, L. Chmielarz, R. L. Alicja, B. Dudek and R. Dziembaj, *Microporous Mesoporous Mater.*, 2005, **78**(1), 11–22.
28 F. Rouquerol, J. Rouquerol and K. Sing, *Adsorption by Powders and Porous Solids*, Academic Press, London, 1999, pp. 219–236.
29 K. S. W. Sing, *Pure Appl. Chem.*, 1985, **54**(11), 2201–2218.
30 L. Deng, Z. Shi, L. Wang and S. Q. Zhou, *J. Phys. Chem. Solids*, 2017, **104**, 79–90.
31 M. Hadnadjev, T. Vulic, R. Marinkovic-Neducin, Y. Suchorski and H. Weiss, *Appl. Surf. Sci.*, 2008, **254**, 4297–4302.
32 S. He, Y. F. Zhao, M. Wei and X. Duan, *Ind. Eng. Chem. Res.*, 2011, **50**(5), 2800–2806.
33 P. Cai, H. Zheng, C. Wang, H. Ma, J. Hu, Y. Pu and P. Liang, *J. Hazard. Mater.*, 2012, **213**, 100–108.
34 K. H. Goh, T. T. Lim and Z. L. Dong, *Water Res.*, 2008, **42**(6–7), 1343–1368.
35 X. X. Guo, F. Z. Zhang, G. Q. Pen, S. L. Xu, X. D. Lei, D. G. Evans and X. Duan, *Chem. Eng. J.*, 2011, **166**, 81–87.
36 S. Kaneko and M. Ogawa, *Appl. Clay Sci.*, 2013, **75**, 109–113.

37 N. K. Lazaridis and D. D. Asouhidou, *Water Res.*, 2003, **37**(12), 2875–2882.
38 Minystry of Environmental Propection of the People's Republic of China, *Integrated Wastewater Discharge Standard GB8978-1996*, Standards press of china, Beijing, 1996.
39 N. Öztürk and T. E. Köse, *Desalination*, 2008, **223**(1–3), 174–179.
40 Y. M. Hao, M. Chen and Z. B. Hu, *J. Hazard. Mater.*, 2010, **184**(1–3), 392–399.
41 M. Islam and R. Patel, *Desalination*, 2010, **256**(1–3), 120–128.